A&A 414, 699–706 (2004)
DOI: 10.1051/0004-6361:20031671

Astronomy & Astrophysics

Library of flux-calibrated echelle spectra of southern late-type dwarfs with different activity levels⋆

C. Cincunegui⋆⋆ and P. J. D. Mauas⋆⋆⋆

Instituto de Astronomía y Física del Espacio, CC. 67, suc. 28, 1428 Buenos Aires, Argentina
Visiting Astronomers, Complejo Astronómico El Leoncito operated under agreement between the Consejo Nacional de Investigaciones Científicas y Técnicas de la República Argentina and the National Universities of La Plata, Córdoba and San Juan

Received 24 April 2003 / Accepted 7 October 2003

Abstract. We present Echelle spectra of 91 late-type dwarfs, of spectral types from F to M and of different levels of chromospheric activity, obtained with the 2.15 m telescope of the CASLEO Observatory located in the Argentinean Andes. Our observations range from 3890 to 6690 Å at a spectral resolution from 0.141 to 0.249 Å per pixel ($R = \lambda/\delta\lambda \approx 26\,400$). The observations were flux calibrated with the aid of long slit spectra. A version of the calibrated spectra is available via the World Wide Web†.

Key words. atlases – stars: late-type

1. Introduction

Spectral libraries of late-type stars are available for different purposes, and therefore with differing properties. For example, for spectral synthesis of the stellar population of galaxies, a homogeneous and complete library with large spectral range is needed, but the spectral resolution is of only secondary concern. One of the libraries with better spectral resolution used for that purpose is the one by Serote Roos et al. (1996), with only a 1.25 Å resolution.

This resolution, however, is much lower than needed for studies of chromospheric activity. In fact, stellar activity is seen only in the cores of the strongest transitions, which usually fill-in, and only in the most extreme cases go into emission.

Only a few high and mid-resolution libraries of spectra of late-type stars are available. The most relevant for activity studies are the ones by Montes et al. (1997, 1999) and Montes & Martin (1998). However, these libraries were published to be used for spectral subtraction, and are therefore limited to the least active stars.

On the other hand, the large database by Prugniel & Soubiran (2001) does not include the spectral region of the Ca II H and K lines, fundamental for studies of stellar activity. Furthermore, this library does not include dM stars, which are interesting for this kind of work, since the dMe stars show the largest chromospheric line emission observed. Moreover, very large flares are observed in several of these stars, and therefore spectra of their quiescent state can be very useful for stellar flare studies.

Furthermore, these libraries are not flux calibrated (in the last one only the low dispersion spectra are calibrated), which limits its utility for several studies like, for example, to investigate the correlation between different flux indices. Finally, all these libraries are composed of northern stars, due to the large number of two-meter-class telescopes in the northern hemisphere. To our knowledge, no library of spectra of southern dwarfs is available to date.

In this paper we present a library of high resolution echelle spectra of southern late-type dwarfs, covering the range from F6 to M5, and of different levels of activity. In particular, we include some flare stars with very large Ca II H and K fluxes. These observations were performed as part of a long term project to study variability of stars.

The spectra covers the wavelength range between the Ca II H and K lines on the blue side, and H_α on the red one, which are the most widely used indicators of stellar activity.

Send offprint requests to: C. Cincunegui,
e-mail: carolina@iafe.uba.ar

⋆ Table 2 is also available in electronic form at the CDS via anonymous ftp to cdsarc.u-strasbg.fr (130.79.128.5) or via http://cdsweb.u-strasbg.fr/cgi-bin/qcat?J/A+A/414/699

⋆⋆ Fellow of the CONICET. e-mail: carolina@iafe.uba.ar
⋆⋆⋆ Member of the Carrera del Investigador Científico, CONICET. e-mail: pablo@iafe.uba.ar

† The spectra are available as FITS and ascii-files at the URL: http://www.iafe.uba.ar/cincunegui/spectra/Table2.html. They are also available in electronic form at the CDS via anonymous ftp to cdsarc.u-strasbg.fr (130.79.128.5) or via http://cdsweb.u-strasbg.fr/cgi-bin/qcat?J/A+A/414/699. When converting the fits to ascii, the spectra were oversampled to a constant $\delta\lambda \approx 0.15$ Å.

Table 1. Observed standard stars.

HR	Spectral type
718	B9 III
1996	O9 V
3454	B3 V
4468	B9.5 V
4963	A1 IV
5501	B9.5 V
7596	A0 III
8634	B8 V
9087	B7 III

In the near future, we plan to incorporate the segment covering the Ca II IRT lines and the He 10830 Å line.

2. The data

2.1. Observations

Our observations were made at the 2.15 m telescope of the Complejo Astronómico El Leoncito (CASLEO), which is located at 2552 m above sea level, in San Juan, Argentina. The library is composed of high-resolution echelle spectra obtained with a REOSC spectrograph designed to work between 3500 and 7500 Å and a 1024×1024 pixel TEK CCD as detector. The maximum wavelength range of our observations is from 3860 to 6690 Å in 24 echelle orders. The spectral resolution ranges from 0.141 to 0.249 Å per pixel ($R = \lambda/\delta\lambda \approx 26\,400$).

Since we do not flux-calibrate the echelle spectra directly, we chose a relatively narrow slit (between 200 and 300 μ) to improve the spectral resolution, despite the loss of some flux.

Due to the strong blaze function of the echelle, it was very difficult to flux calibrate the high-resolution spectra directly. Therefore, for each program star we obtained a medium-resolution long-slit spectrum which we used for the calibration as explained in Sect. 2.3.

The long-slit spectra were obtained with the same spectrograph, replacing the echelle grid by a mirror. The spectral resolution is ≈3.4 Å per pixel ($R \approx 1050-2070$ in the observed range 3500−7000 Å). In this configuration we broadened the slit to 400 μ to assure photometric conditions.

The observations presented here were obtained in three observing runs in 2002. The first was between March 29 and April 1st, the second between August 11 and 14, and the last one between November 21 and 24. In all cases, the first three nights were devoted to the echelle observations, and the last one to the long slit ones. More spectra will be added in the future, as they are obtained and processed.

2.2. Data reduction: The long-slit spectra

The long-slit spectra were reduced following the standard procedure. We checked the accuracy of the flat-field images, and decided not to use them because of the noise they introduced.

Besides the program stars, we observed 9 spectrophotometric standards, listed in Table 1, which were processed following the same procedure as the program stars. To check the photometric conditions, we flux-calibrated each standard star with all the others, and obtained in all cases fluxes within 10% of the ones listed in the IRAF[1] database. We then flux calibrated each long-slit program spectra with the closest standard star observed, using the standard IRAF routines.

2.3. Data reduction: The echelle spectra

For each star in the sample we took two echelle spectra. On the one hand, this helped us to remove cosmic rays. On the other hand, one should keep in mind that some of these stars show very frequent flares. Since this is the case particularly for the weaker dMe stars, for which integration times as large as two hours are needed, there is a definite possibility of observing a flare and therefore overestimating the activity of the star. The echelle spectra of both images were optimally extracted and wavelength calibrated using IRAF. We visually inspected the Ca II line region of both spectra, and did not find any strong variability. Then we combined both spectra removing cosmic rays.

The blaze function superimposed in each spectroscopic order was too pronounced to normalize the spectra. We flux calibrated each order of the echelle spectra separately according to the following procedure.

First, we reduced the resolution of the flux-calibrated long-slit spectra to 13.69 Å (corresponding to 4 pixels), in order to increase the signal-to-noise ratio. These re-sampled program spectra were then used to obtain a sensitivity function with the usual IRAF routines for each order of each program star. We used these sensitivity functions to calibrate each order.

When we calculated this sensitivity function, we took special care with the strongest spectral lines, which are of particular interest for activity studies. Since a small difference in the sensitivity function can strongly affect the strength of the lines, in many cases we had to eliminate several pixels from the fit of the sensitivity function.

Finally, we combined the flux-calibrated echelle orders to obtain a one-dimensional spectrum. We eliminated the extremes of the orders where the signal-to-noise ratio was poor and averaged the remaining overlapping regions of subsequent orders.

As a final step, we integrated the flux to obtain a V magnitude and, when needed, rescaled our observations to the V listed in Table 2 below.

In Fig. 1 the flux-calibrated long-slit and the echelle spectra are shown for HD 158614, over the whole spectral range. To appreciate the good agreement between both spectra, in Fig. 2 we present on a detailed wavelength scale the echelle spectrum re-sampled to 6.85 Å, which corresponds to 2 pixels of the the long-slit spectrum, which is also shown.

[1] The Image Reduction and Analysis Facility (IRAF) is distributed by the Association of Universities for Research in Astronomy, Inc., under contract to the National Science Foundation.

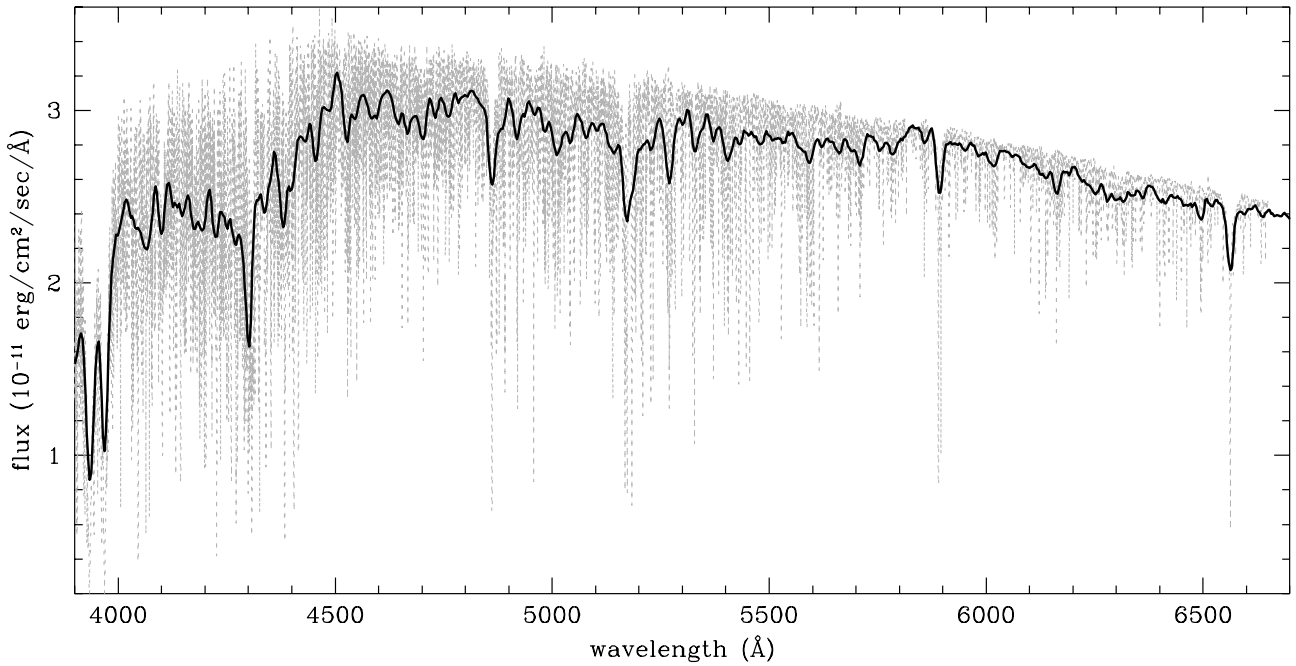

Fig. 1. The low resolution spectrum (solid line), superimposed on the high resolution spectrum (dotted line), for HD 158614. The whole wavelength range of the spectra are shown.

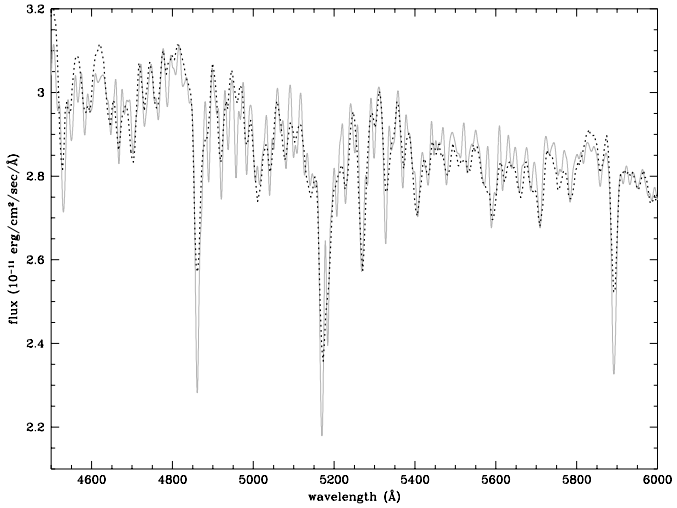

Fig. 2. The high resolution spectrum re-sampled to 6.85 Å (full line) and the low resolution spectrum (dotted line). The star is the same that in Fig. 1.

3. The library

In Table 2 we list the stars included in the library. For each star we give the HD and GJ numbers and the star name in the three leftmost columns. In the fourth column we specify which stars are expected to be very active, either because they are dMe stars (with the Balmer lines in emission), or because they belong to the RS CVn or the BY Dra types. In that column we also specify which stars were chosen as non-variable by Duncan et al. (1991), based on the long term database of Mount Wilson observations of the Ca II lines. Also indicated are the stars for which planetary systems have been reported.

In the fifth to tenth columns we list the star's spectral type, its V magnitude, $B - V$ and $U - B$ colors, metallicity (from Cayrel de Strobel et al. 1997, 2001) and trigonometric parallax, from "The Hipparcos and Tycho Catalogue" (ESA 1997), except the ones indicated.

For these active stars, it is important to assess both the activity level and the variability. With this in mind, we include in the table the most widely used index of activity, the S index used at Mount Wilson Observatory, which is defined as the ratio between the flux in the center of the Ca II H and K lines to the continuum nearby. For those stars that have been observed at Mount Wilson, we give in Cols. 11 and 12 both the minimum and maximum values of S that have been observed over the years (from Duncan et al. 1991). For those southern stars that were observed at Cerro Tololo by Henry et al. (1996), we list their value in Col. 13. We also list in Col. 14 the value obtained from our spectra, after the calibration explained in Cincunegui & Mauas (2002) is performed, using the stars indicated with § in the table. Finally, we also include the date in which the observation was performed.

Several of our spectra for different spectral type stars are shown in Fig. 3. The low and high resolution flux-calibrated spectra are available via the World Wide Web. Also available through the web is Table 2.

4. Discussion

18 of our stars were also observed by Prugniel & Soubiran (2001). Although in most cases their spectra and ours agree very well, we noted some differences for a few stars. For example, in Fig. 4 we compare their spectrum for HD 9562 with ours (the two lowermost spectra in each panel). To check whether the difference was due to an error in our calibration, we

Table 2. Observed stars.

HD	GJ	Name		Spectral type	V	$B-V$	$U-B$	[Fe/H]	Parall.	S_{MW} min	S_{MW} max	S_{CTIO}	S_{CM}	Date
1835	17.3	BE Cet	§‡	G3 V	6.38	0.67	0.22	−0.01	49.05	0.283	0.439	0.344	0.35	09.01.02
3405	24A			G0/1 V	6.78	0.64			22.79				0.38	11.23.02
3443	25		§	K1 V	5.57	0.71	0.20	−0.16[a]	64.38	0.149	0.782	0.185	0.18	11.23.02
3795	27.2		§	G3/5 V	6.14	0.70	0.21	−0.70	35.02	0.137	0.171	0.145	0.16	11.23.02
4308	31.5			G5 V	6.54	0.65	0.12	−0.47	45.76			0.152	0.17	11.21.02
9562	59.2		§	G2 IV	5.76	0.60	0.24	0.18	33.71	0.113	0.155	0.146	0.14	11.23.02
10700	71	tau Cet	§	G8 V	3.50	0.72	0.22	−0.59	274.18	0.161	0.185	0.171	0.18	11.21.02
11131	9061B	chi Cet B	§	G0	6.72	0.60	0.12	−0.06	43.47			0.310	0.36	11.21.02
13445	86		⋆	K1 V	6.17	0.77		−0.21	91.63			0.251	0.31	11.21.02
16673	3175		§	F6 V	5.80	0.47	0.03	−0.01	46.42	0.173	0.243	0.229	0.21	09.01.02
17051	108	iot Hor	⋆	G0 V	5.40	0.57		−0.04	58.00			0.225	0.23	11.23.02
17576				G0 V	7.92	0.52			6.13			1.611	0.92	11.23.02
17925	117	EP Eri	§†	K1 V	6.00	0.91	0.55	0.10	96.33	0.523	0.907	0.662	0.70	08.30.02
19034	121.2			G5	8.09	0.67	0.11		28.33				0.17	08.30.02
19467	3200			G3 V	7.00	0.65	0.15		31.76				0.16	08.31.02
19994	128	94 Cet	⋆	F8 V	5.06	0.57	0.12	0.15	44.69				0.17	11.21.02
20619	135			G1.5 V	7.10	0.59	0.09	−0.20	40.52				0.20	08.30.02
20766	136	zet01 Ret		G2.5 V	5.54	0.64	0.08	−0.22	82.51			0.245	0.25	09.01.02
22049	144	eps Eri	§‡	K2 V	3.73	0.88	0.58	−0.14	310.74	0.419	0.642	0.483	0.44	08.31.02
23249	150	del Eri	§‡	K0 IV	3.51	0.92	0.68	0.05	110.58	0.127	0.175	0.129	0.13	08.31.02
26965	166A	DY Eri	§	K1 V	4.41	0.82	0.45	−0.25	198.25	0.176	0.252	0.185	0.17	09.01.02
27442	167.3	eps Ret	⋆	K2 IVa	4.44	1.08	1.07	0.22	54.84				0.11	11.23.02
28246				F6 V	6.39	0.40			27.00				0.20	11.21.02
30495	177	58 Eri	§	G3 V	5.50	0.64	0.13	−0.13	75.10	0.239	0.363	0.286	0.34	09.01.02
32147	183			K3 V	6.22	1.06	0.99	0.34	113.46	0.205	0.399		0.28	11.21.02
35850				F7 V	6.31	0.50		0.00	37.26				0.53	11.23.02
36395	205			M 1.5	7.92	1.52	1.21	0.60[a]	175.72				2.15	09.01.02
37572		UY Pic		K0 V	7.93	0.83						0.952	0.74	08.31.02
38392	216B	gam Lep B	§	K2 V	6.15	0.94	0.74	0.02				0.534	0.41	09.01.02
38393	216A	gam Lep A	§	F7 V	3.60	0.47		−0.12	111.49			0.182	0.17	11.22.02
38858	1085			G4 V	5.97	0.64	0.07		64.25				0.18	11.23.02
39917		SZ Pic	†	G8 V	7.90	0.76			5.13			0.975	0.62	09.01.02
41824			†	G6 V	6.57	0.72	0.34		33.64			0.612	0.62	09.01.02
42581	229A		◂	M1/2 V	8.14	1.51			173.19				1.56	09.01.02
43587	231.1A			F9 V	5.71	0.61	0.08	−0.08	51.76	0.131	0.173		0.16	11.23.02
45067			§	F8 V	5.90	0.53	0.05	−0.16	30.22	0.115	0.167	0.148	0.16	08.31.02
45270				G1 V	6.53	0.56			42.56			0.402	0.42	11.21.02
48189	3400A			G1.5 V	6.18	0.57	0.16		46.15			0.430	0.46	09.01.02
59967	3446			G4 V	6.67	0.60			45.93			0.384	0.41	11.22.02
75289			⋆	G0 I a	6.36	0.58	0.10	0.28	34.55			0.154	0.15	03.29.02
82106	349		◂	K3 V	7.22	1.00	0.90		78.87	0.797	0.797		0.67	03.30.02
94683				K4 V	5.97	1.78	2.01		1.96				0.37	03.31.02
97233	416			K4 V	9.05	1.21	1.08		44.00				0.73	03.29.02
101581	435		◂	K4/5 V	7.77	1.07	0.90		79.91				0.51	03.29.02
103112	3689A			K0	7.54	1.05	0.90		12.39				0.13	03.31.02
105115				K2/3 V	6.90	1.41			2.85				0.11	03.31.02
114762			⋆	F9 V	7.30	0.55	−0.07	−0.82	24.65				0.17	03.29.02
117176	512.1	70 Vir	⋆	G4 V	5.00	0.69	0.26	−0.11	55.22	0.134	0.162		0.15	03.29.02

Table 2. continued.

HD	GJ	Name		Spectral type	V	$B-V$	$U-B$	[Fe/H]	Parall.	S_{MW} min	S_{MW} max	S_{CTIO}	S_{CM}	Date
118100	517	EQ Vir	◃	K5 Ve	9.31	1.20	1.04	−0.15[a]	50.54				3.44	03.30.02
119850	526		◃	M1.5	8.46	1.45	1.09		184.13	0.949	0.949		1.02	03.29.02
120136	527A	tau Boo	⋆	F6 IV	4.50	0.48		0.32	64.12	0.170	0.224		0.22	03.29.02
122303	536			M1	9.72	1.49	1.17		98.26				0.95	03.29.02
125072	542			K3 V	6.66	1.03	0.94	0.26	84.50				0.26	03.29.02
128620	559A	alf Cen A		G2 V	−0.01	0.71	0.22	0.22	742.24			0.162	0.16	08.30.02
128621	559B	alf Cen B		K1 V	1.33	0.88	0.67	0.24	742.22			0.209	0.23	03.29.02
130948	564			G1 V	5.88	0.55	0.00	−0.20	55.73			0.309	0.30	03.29.02
131977	570A			K4 V	5.74	1.11	1.03	0.03	169.31			0.709	0.43	08.31.02
144253	610			K3/4 V	7.40	1.04	0.94	−0.03	53.93				0.21	03.31.02
146233	616	18 Sco		G2 Va	5.50	0.65	0.16	0.05	71.30	0.167	0.186		0.19	03.29.02
147513	620.1A			G5 V	5.38	0.60	0.14	0.03	77.69			0.291	0.32	09.01.02
151770				G3/5 V	8.34	0.65			7.45			1.000	0.71	08.30.02
152391	641	V2292 Oph	§‡	G8 V	6.64	0.76	0.32		59.04	0.278	0.482	0.431	0.40	03.29.02
156026	664	36 Oph C	†	K5 V	6.34	1.16	0.94	−0.21	167.56	0.577	1.084	1.188	0.73	08.31.02
156425				K4 V	7.88	1.94		−0.20	−0.32				0.31	03.31.02
157881	673			K5	7.54	1.36	1.27	−0.20	129.54	1.452	1.475		1.76	08.30.02
158614	678		§	G9 IV-V	5.31	0.72	0.31	−0.05	60.80	0.144	0.180	0.168	0.17	08.31.02
160691	691	mu Ara		G3 IV-V	5.15	0.70	0.23	0.20	65.46			0.159	0.15	03.29.02
165185	702.1			G5 V	5.95	0.57	0.12	−0.06	57.58			0.333	0.33	03.29.02
172051	722			G5 V	5.87	0.63	0.17		77.02			0.181	0.19	03.30.02
173560	725.3			G3/5 V	8.67	0.62	0.14		11.65				0.18	03.29.02
177996	4096			K1 V	7.88	0.86	0.53		31.48			0.861	0.50	03.29.02
180617	752A		◃	M2.5	9.13	1.50	1.15		170.25	1.050	1.453		1.12	03.31.02
187923	4126			G0 V	6.10	0.68	0.13	−0.20	36.15				0.15	03.29.02
188088	770	V4200 Sgr	‡	K3/4 V	6.18	1.02	0.96		70.34				0.59	03.30.02
189567	776			G3 V	6.07	0.64	0.07	−0.30	56.45			0.185	0.17	03.29.02
197076	797A			G5 V	6.45	0.63	0.09		47.65	0.158	0.180		0.19	08.31.02
197214	4157			G5 V	6.95	0.67			44.57			0.188	0.32	11.22.02
202628	825.2			G2 V	6.75	0.63	0.14	−0.14	42.04			0.217	0.26	11.22.02
202917				G5 V	8.67	0.65			21.81			0.743	0.76	11.23.02
209100	845	eps Ind	◃	K4.5 V	4.69	1.06	0.99	−0.23	275.79			0.668	0.40	11.22.02
210918	851.2			G5 V	6.26	0.62	0.14	−0.18	45.19			0.168	0.16	11.23.02
212330	857			G3 IV	5.31	0.68	0.13	−0.04	48.81			0.149	0.16	08.31.02
213941	863.3			G5 V	7.59	0.66	0.12	−0.42	30.98			0.181	0.20	11.23.02
215768				G0 V	7.50	0.55			25.34			0.318	0.33	08.31.02
219834	894.2A	94 Aqr	§	G6/8 IV	5.19	0.79	0.41	0.09	33.00[b]	0.139	0.181	0.145	0.16	11.23.02
225213	1			M1.5	8.57	1.46	0.96		229.32				0.33	08.31.02
	375	LU Vel	◃	M3.5	11.27	1.56	0.91		62.88				4.68	03.30.02
	388	AD Leo	◃	M3.5 V	9.43	1.54	1.08		213.00[b]				9.23	03.29.02
	479			M2	10.64	1.57	1.14		103.54				2.10	03.31.02
	551	Proxima Cen	◃	M5.5 Ve	11.05	1.97	1.43		772.33				16.91	09.01.02
	699	Barnard's	◃	M4 Ve	9.54	1.74	1.29		549.30				0.99	09.01.02

Notes: ⋆: stars with planets.

§: stars reported in CTIO as non-variable, which were used to calibrate the S indexes in Cincunegui & Mauas (2002).

◃: dMe stars, or stars presumably active.

†: RS CVn type.

‡: BY Dra type.

[a] from Cayrel de Strobel et al. (1997); the rest from Cayrel de Strobel et al. (2001).

[b] from Jenkins (1952); the rest from "The Hipparcos and Tycho Catalogue" (ESA 1997).

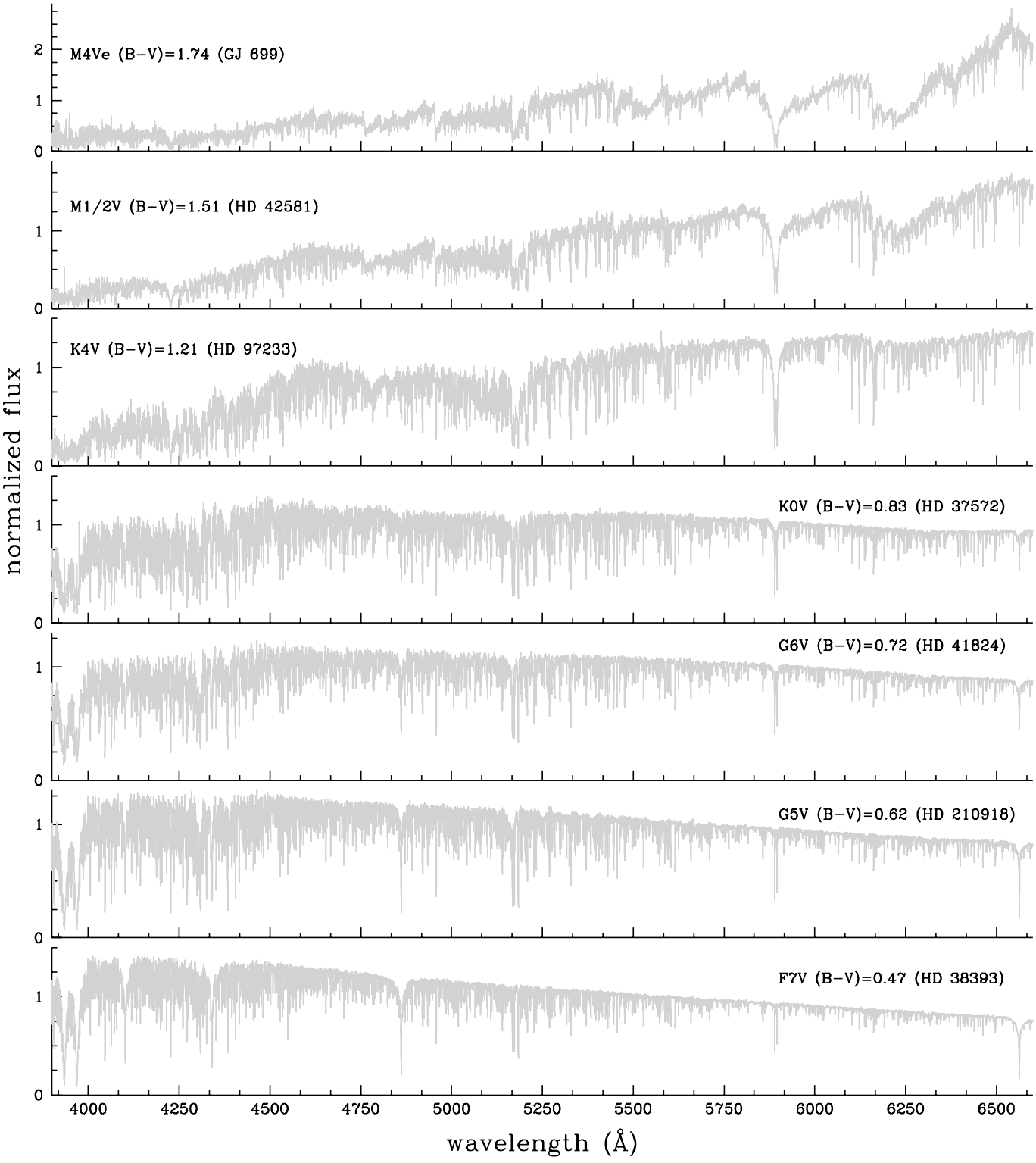

Fig. 3. Some spectra of stars of different types. In each case the spectral type, the colour index and the name of the star is indicated. For a better comparison, the spectra are normalized to flux 1 in the *V* filter.

compare a lower resolution spectrum for a star of the same spectral type, taken from Silva & Cornell (1992) with ours resampled to this lower resolution (the two uppermost spectra). We see that these last spectra are practically identical. We have compared all our spectra with both quoted libraries, finding differences smaller than 10% in most cases.

As an example of the differences in spectra that can be found between stars of the same spectral type but different levels of activity, in Figs. 5 to 7 we compare several of the solar-type stars included in our sample, with the Solar flux from the FTS atlas by Brault and Neckel (Neckel 1999), resampled to our resolution. In Fig. 5, the wavelength range is chosen to

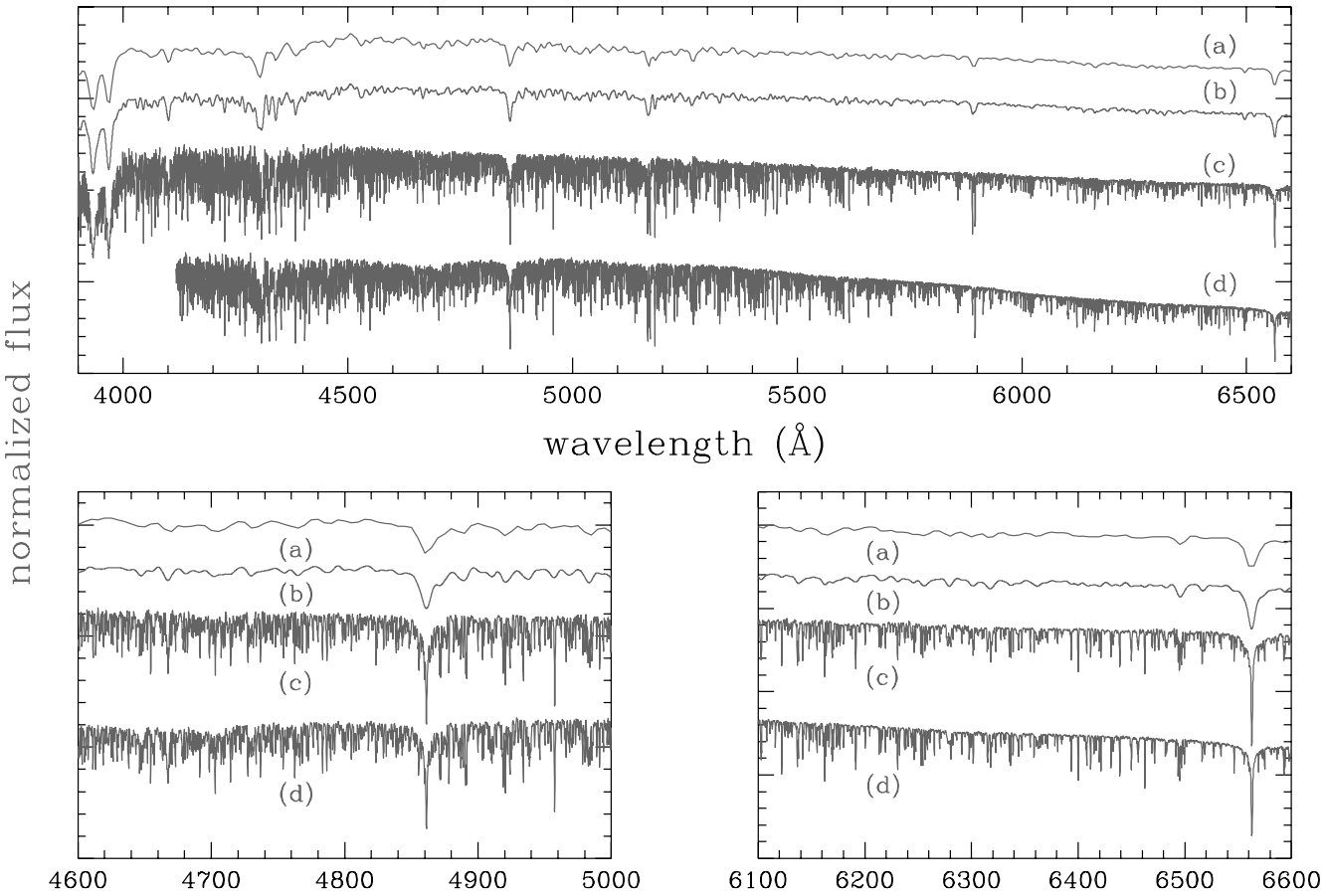

Fig. 4. In the upper panel, we compare our spectrum for HD 9562 (labeled c) with the spectrum of the same star from Prugniel & Soubiran (2001), resampled to our resolution (labeled d). Also shown, is a spectrum for a star of spectral type G2 IV and $B - V = 0.62$ from Silva & Cornell (1992, labeled a) and ours resampled to the same resolution (labeled b). The flux is normalized as in Fig. 3, and the four spectra are arbitrarily displaced for clarity. In the lower panels, we show details of two spectral regions.

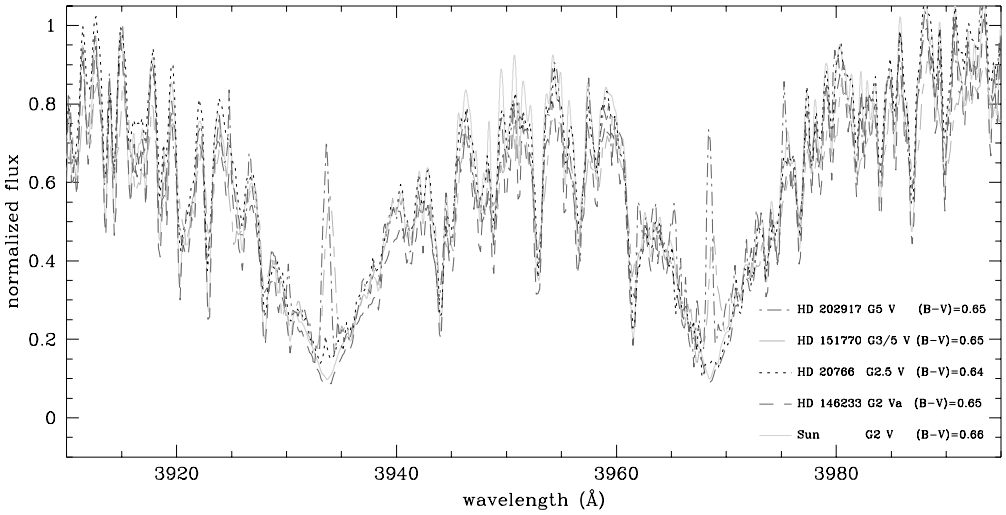

Fig. 5. Several of our solar-type stars and the Sun: the Ca II H and K region. For a better comparison, the spectra are normalized to flux 1 in the *V* filter.

show the Ca II lines, which are, as previously discussed, the most widely used proxy of chromospheric activity, while in Figs. 6 and 7 we show the Na I *D* doublet and the H_α line region. As expected, the photospheric contribution for all the stars is practically the same, while the cores of the lines are different, showing that these stars have a very similar photosphere but their levels of activity differ.

Acknowledgements. We would like to thank the director of the CASLEO Observatory, Dr. H. Levato, and all the staff of this institution, for their invaluable help. We also thank Dra. Nidia Morrell for

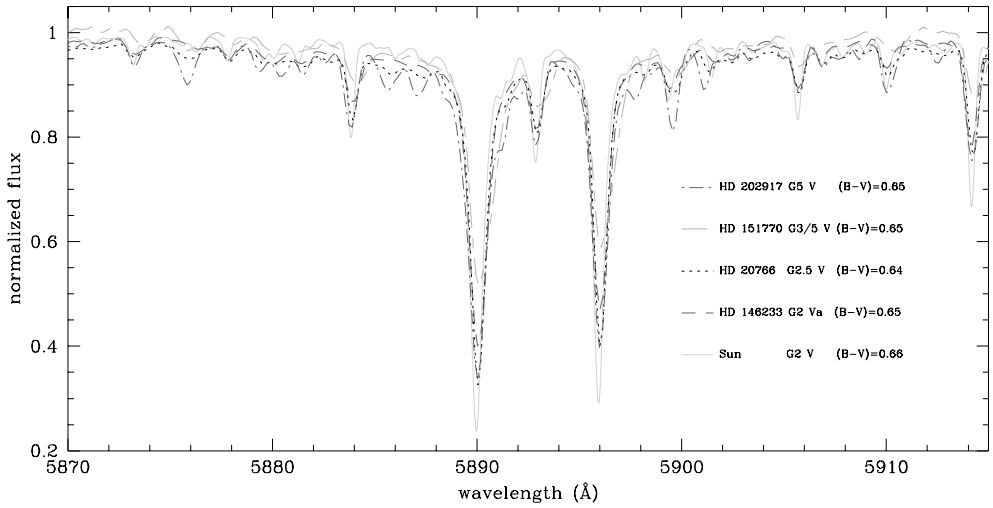

Fig. 6. Several of our solar-type stars and the Sun: the Na I *D* doublet region. For a better comparison, the spectra are normalized to flux 1 in the *V* filter.

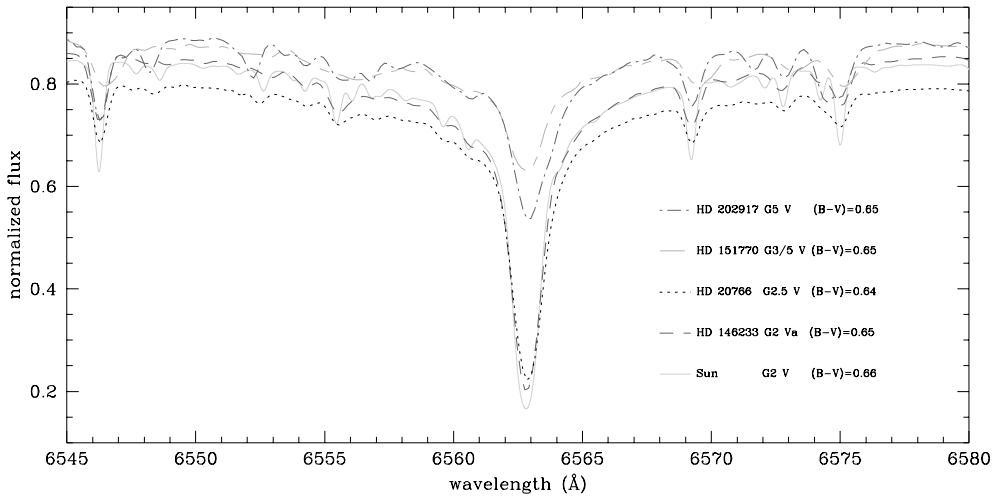

Fig. 7. Several of our solar-type stars and the Sun: the H_α region. For a better comparison, the spectra are normalized to flux 1 in the *V* filter.

her useful advise, and the unknown referee for many useful comments. The CCD and data acquisition system at CASLEO has been partly financed by R. M. Rich through US. NSF grant AST-90-15827. This work made extensive use of the SIMBAD database, operated at CDS, Strasbourg, France.

References

Cayrel de Strobel, G., Soubiran, C., Friel, E. D., Ralite, N., & Francois, P. 1997, A&A, 124, 299

Cayrel de Strobel, G., Soubiran, C., & Ralite, N. 2001, A&A, 373, 159

Cincunegui, C., & Mauas, P. J. D. 2002, in ESA SP-477, 91

Duncan, D. K., Vaughan, A. H., Wilson, O. C., et al. 1991, ApJS, 76, 383

ESA 1997, The Hipparcos and Tycho Catalogues, ESA SP–1200

Henry, T. J., Soderblom, D. R., Donahue, R. A., & Baliunas, S. L. 1996, AJ, 111, 439

Jenkins, L. F. 1952, General Catalogue of Trigonometric Stellar Parallaxes, compiled at the Yale Univ. Obs.

Montes, D., & Martin, E. L. 1998, A&AS, 128, 485

Montes, D., Martin, E. L., Fernández-Figueroa, M. J., Cornide, M., & de Castro, E. 1997, A&AS, 123, 473

Montes, D., Ramsey, L. W., & Welty, A. D. 1999, ApJS, 123, 283

Neckel, H. 1999, Sol. Phys., 184, 421

Prugniel, P., & Soubiran, C. 2001, A&A, 369, 1048

Serote Roos, M., Boisson, C., & Joly, M. 1996, A&A, 117, 93

Silva, D. R., & Cornell, M. E. 1992, ApJS, 81, 865